

Surface Brightness of Starbursts at Low and High Redshifts

Daniel W. Weedman

Department of Astronomy and Astrophysics, 525 Davey Laboratory, The Pennsylvania State University, University Park, PA 16802

Jeffrey B. Wolovitz

Department of Astronomy and Astrophysics, 525 Davey Laboratory, The Pennsylvania State University, University Park, PA 16802

Matthew A. Bershadly

Department of Astronomy, 475 North Charter St., University of Wisconsin, Madison, WI 53706

Donald P. Schneider

Department of Astronomy and Astrophysics, 525 Davey Laboratory, The Pennsylvania State University, University Park, PA 16802

ABSTRACT

Observations in the rest frame ultraviolet from various space missions are used to define the nearby starburst regions having the highest surface brightness on scales of several hundred pc. The bright limit is found to be 6×10^{-16} ergs $\text{cm}^{-2} \text{s}^{-1} \text{\AA}^{-1} \text{arcsec}^{-2}$ for rest frame wavelength of 1830 \AA . Surface brightness in the brightest pixel is measured for 18 galaxies in the Hubble Deep Field having $z > 2.2$. After correcting for cosmological dimming, we find that the high redshift starbursts have intrinsic ultraviolet surface brightness that is typically four times brighter than low redshift starbursts. It is not possible to conclude whether this difference is caused by decreased dust obscuration in the high redshift starburst regions or by intrinsically more intense star formation. Surface brightness enhancement of starburst regions may be the primary factor for explaining the observed increase with redshift of the ultraviolet luminosity arising from star formation.

Subject headings: galaxies: evolution — galaxies: distances and redshifts — galaxies: starbursts

1. Introduction

Many new observational results make possible investigations of the evolution of star formation within galaxies, extending to redshifts approaching four (Madau *et al.* 1996, Lilly *et al.* 1996, Connolly *et al.* 1997). To date, the essence of these results is that the global star forming rate, deduced from the ultraviolet luminosity integrated over all observable galaxies in co-moving volumes of the universe, was significantly greater at earlier epochs than it is today. These results describe the overall rate of star formation. This star formation is in “starbursts” for those galaxies whose appearance is dominated by short-lived populations of young stars. While counts of such star-forming galaxies can determine global rates, these results do not address the question of whether the local characteristics of the star formation process within individual galaxies also depends on epoch in the universe. Understanding these characteristics of star formation is crucial to explaining the changing rate of star formation with epoch.

Recent dramatic progress in identifying starburst galaxies at redshifts above two in the Hubble Deep Field (Steidel *et al.* 1996, Lowenthal *et al.* 1997) has produced a sample of such galaxies that can be examined with sufficient spatial resolution that individual starburst regions can be examined within the galaxies. For the first time, it becomes possible to compare such regions with those of similar size in nearby galaxies and to make this comparison in the rest-frame ultraviolet luminosity, which originates completely from the starburst. This allows an initial comparison of the starburst process between galaxies separated in time by amounts exceeding two-thirds the age of the universe.

2. Surface Brightnesses of Starburst Regions

Our objective in the present analysis is a direct comparison between the surface brightness of starburst regions at low redshift and at high redshift, as observed in the rest frame ultraviolet where the luminosity is completely dominated by the recently formed stars. If the starburst region is resolved, surface brightness is a very useful parameter for comparing regions of greatly differing redshift; surface brightness, unlike luminosity or diameter, does not depend on cosmological parameters, i.e. H_0 , Ω_0 or Λ_0 . This makes possible a comparison of local physical conditions that is independent of cosmological assumptions.

In Euclidean space, surface brightness is independent of distance. For significant redshifts, surface brightness changes dramatically but only in terms involving $(1+z)$. When measured in f_λ units at a given rest-frame wavelength, distant objects of the same intrinsic

surface brightness should have their observed surface brightness fade by $(1+z)^{-5}$ for Friedmann cosmologies. There are five factors of $(1+z)$ when observations are in f_λ units; two factors because of the change in unit area observed from the galaxy, one for change in unit time, one for change in photon energy, and one for change in unit wavelength bandpass. (If observations are in bolometric quantities, such as λf_λ or νf_ν units, only the first four factors of $(1+z)$ enter. This is equivalent to observing in a band-pass fixed in either the observed or rest frame. If counting photons, there is still one less factor of $(1+z)$.)

Achieving a surface brightness measurement requires that the starburst regions be resolved. We refer to these resolved sources as “extended starburst regions”. We avoid starbursts associated with galactic nuclei, because the starburst luminosity in such cases may be confused with that of an unresolved active galactic nucleus. An empirical upper limit to the rest frame ultraviolet surface brightness of such regions within nearby galaxies is deduced by searching for those nearby extended starburst regions with the highest surface brightness. Observations in the ultraviolet from a variety of space missions are the source of the relevant data. These results are summarized in Table 1. The galaxies observed with the various missions were chosen as sources expected to be ultraviolet-bright. While it is possible that even brighter extended starburst regions have been overlooked, the similarity in the results from independent selections of galaxies gives reasonable confidence that a meaningful upper limit for surface brightness of extended starburst regions in nearby galaxies can be determined from these various observations.

An extensive compilation of observations of star-forming galaxies with the International Ultraviolet Explorer (IUE) is given by Kinney et. al. (1993). For many such observations, the starburst regions are significantly smaller than the $10'' \times 20''$ IUE aperture, so surface brightnesses within this aperture are underestimates (ultraviolet images of some nearby galaxies from the HST Faint Object Camera are in Maoz et al. 1996). Not surprisingly, the brightest such galaxies within an aperture this large are generally also the closest, for which the starbursts would be resolved by the IUE aperture. Excluding NGC 1068, the five galaxies with brightest total flux at 1900 Å (their 1863-1963 Å bandpass) are NGC 1705, 3310, 4449, 5236, and 5253. The average surface brightness of these five, with the IUE aperture taken as 200 arcsec^2 , is $5 \times 10^{-16} \text{ ergs cm}^{-2} \text{ s}^{-1} \text{ Å}^{-1} \text{ arcsec}^{-2}$. Defining the scale size by the $20''$ length of the aperture, these brightnesses arise from regions of average size 700 pc. While it is arbitrary to restrict our selection to the five brightest, it can be seen from Table 1 that any other entries would be more than a factor of two fainter than the brightest of all (NGC 5236).

The galactic disk with highest observed ultraviolet surface brightness is the inner disk of NGC 1068, characterized by extensive star formation throughout the 3 kpc diameter

disk centered on the active nucleus of this prototype Seyfert 2 galaxy. Numerous individual bright regions were imaged with the Ultraviolet Imaging Telescope on the Astro 1 mission (Neff *et al.* 1994). The brightest of these is their knot complex labeled “region J”, stated to have flux at 1500 Å of 2×10^{-14} ergs cm⁻² s⁻¹ Å⁻¹. From their published image, this region appears dominated by bright knots covering an area of about 30 arcsec², which yields a surface brightness of 7×10^{-16} ergs cm⁻² s⁻¹ Å⁻¹ arcsec⁻², within a characteristic diameter of about 350 pc (5'' at an assumed distance of 15 Mpc for $H_0 = 75$ km s⁻¹ Mpc⁻¹; this value of H_0 is assumed throughout).

Several starburst galaxies were imaged at 2200 Å with the Faint Object Camera of the Hubble Space Telescope (Meurer *et al.* 1995). Among these is the highly luminous and well studied starburst galaxy NGC 3690 (Markarian 171). The brightest uv knot, NGC 3690-BC, has surface brightness of 5×10^{-16} ergs cm⁻² s⁻¹ Å⁻¹ arcsec⁻² within diameter of 6.4'' (1360 pc at distance 44 Mpc).

For comparisons to follow with starburst regions at high redshift, we desire a normalizing wavelength of 1830 Å. Nominal corrections to the observed values in Table 1 are applied by assuming a common spectral shape for all objects observed. Taking the median starburst ultraviolet spectral shape from Kinney *et al.* (1993) of $f_\lambda \propto \lambda^{-1}$, the rest-frame surface brightnesses at 1830 Å are also tabulated. The results are adequately consistent to define a meaningful measure of the surface brightness for the brightest local starbursts. Using these results, we adopt a value of 6×10^{-16} ergs cm⁻² s⁻¹ Å⁻¹ arcsec⁻² for the surface brightness of the “brightest” starburst regions within nearby starbursts when observed at a rest frame wavelength of 1830 Å. We will use this number with which to compare the observed surface brightness of systems at high redshift.

The image quality of HST allows star forming regions to be resolved, and surface brightnesses to be measured, even to the highest observable redshifts. In the Hubble Deep Field (Williams *et al.* 1996), the “drizzled add” pixels are 0.04'' in size. Such a pixel corresponds to a physical size of about 300 pc at $2 < z < 3$ (for $\Omega_0 = 0.2$; angular sizes change little with redshift for this Ω_0 and $\Lambda_0 = 0$). This is sufficiently small compared to the size of luminous starburst regions in nearby galaxies (Table 1) that it is meaningful to compare surface brightnesses of distant starbursts in the HDF with those in nearby galaxies. Although spatial resolution in the HDF as defined by the point spread function is larger than the size of a single pixel, the surface brightness measures from a single pixel are accurate measures if starburst regions are fully resolved in the HDF. If the starburst regions are unresolved, a measure of the surface brightness in the brightest pixel provides a lower limit to the actual surface brightness of the source within an area of 0.016 arcsec². The surface brightness would be higher if the source is smaller than a single pixel and

is unresolved. In such cases, however, the starburst regions at high redshift would be significantly smaller than most of the nearby regions in Table 1. Because of smearing by the point spread function, measuring surface brightness in the brightest pixel does not yield a value that is significantly greater than an average taken over a few pixels. The brightest pixel is typically found to be a factor of 1.09 times brighter than the average of the four brightest pixels (600 pc at $2 < z < 3$) and 1.22 times brighter than the average of the nine brightest (900 pc at $2 < z < 3$). These apertures are comparable to the IUE, HST FOC, and UIT apertures used to measure the surface brightness of the local starbursts listed in Table 1.

There are 18 galaxies in the HDF with known redshifts sufficiently high that rest-frame flux measurements are available for ultraviolet wavelengths comparable to those at which surface brightnesses of local starburst regions have been measured. For these galaxies in the HDF, the ultraviolet surface brightness at 1830 Å rest-frame wavelength is given in Table 2. Objects in this Table have redshifts determined by the authors referenced, using the Keck Telescope. Images of these objects from the HDF are shown in Figure 1. Surface brightness is measured from the single brightest pixel using a linear interpolation between the effective wavelengths of the two filters which flank the redshifted 1830 Å wavelength in the observer’s frame. The brightest pixel is chosen from the F814W image, and the same pixel is used in the F606W or other images to determine the interpolation. The choice of 1830 Å for the comparison wavelength is made so that the object of highest redshift in the analysis has rest wavelength corresponding to an observed wavelength no longer than the effective wavelength of the F814W image.

3. Comparing Low Redshift and High Redshift Starburst Regions

Ultraviolet observations of nearby starburst regions summarized in §2 indicate that the maximum surface brightness of such regions is about 6×10^{-16} ergs cm^{-2} s^{-1} Å^{-1} arcsec^{-2} when observed at a wavelength of 1830 Å. Distant objects of the same intrinsic surface brightness should have their observed surface brightness, at the same rest-frame wavelength, reduced to $6 \times 10^{-16} (1 + z)^{-5}$ ergs cm^{-2} s^{-1} Å^{-1} arcsec^{-2} .

Figure 2 displays the observed surface brightnesses at the rest frame wavelength of 1830 Å (observer’s wavelength of $1830(1 + z)$ Å) from the HDF starburst regions in Table 2. These are compared to the expected surface brightness from the scaling from low redshift starbursts. As expected from the cosmological fading, surface brightnesses of high redshift starbursts are dramatically less than for starburst regions at low redshifts. Nevertheless, objects in the HDF with high redshifts have rest-frame surface brightnesses significantly

greater than expected using the scaling from local starbursts. From Figure 2, the median excess is a factor of 4, and the brightest starburst in the Figure exceeds the expected surface brightness *by a factor of 11*. Keeping in mind that these values are only lower limits if starburst regions are smaller than a single pixel, this result clearly demonstrates that galaxies at high redshift detected in the HDF have higher ultraviolet luminosity per unit area than the brightest known examples of local starbursts.

This is a different conclusion from that of Meurer *et al.* (1997) and Pettini *et al.* (1998). These authors conclude from ultraviolet surface brightnesses that starburst regions have similar star formation intensity per unit area regardless of redshift. Pettini *et al.* state that starburst regions at high redshift are “spatially more extended versions of the local starburst phenomenon.” Differences between our conclusions and theirs may arise primarily because we measure surface brightnesses within the smallest observable spatial scales, using the closest starburst regions for comparisons and using only starbursts from the HDF to deduce the surface brightness of the starburst regions at high redshift. Their results refer to spatial scales at high redshift averaged over half-light radii of about 2000 pc, which are significantly larger scales than those within which we measure surface brightnesses.

The difference in our comparison between low redshift and high redshift starburst regions is not explainable simply as a selection effect arising from comparing significantly different volumes of space. If a much larger co-moving volume of the universe were observed to locate starbursts in the HDF compared to the volume of space used to locate the low redshift comparison starbursts, it might be expected that rarer, brighter regions would define the brightest examples in the larger volume. Consider the volume examined to find the high redshift starbursts in the HDF. There are 18 galaxies in Table 2, distributed roughly evenly in redshift for $2.2 < z < 3.4$, and 17 of these galaxies exceed the surface brightness of the local starburst galaxies. The three WF CCDs of the HDF examined to find these galaxies cover 1.5×10^{-3} deg². Within this area of the sky, the co-moving volume increment in this redshift range is 15×10^4 Mpc³ (for $\Omega_0 = 0.2$) or 5×10^4 Mpc³ (for $\Omega_0 = 1$). These alternative volumes yield volume densities of the brightest high redshift starbursts between 11×10^{-5} Mpc⁻³ and 34×10^{-5} Mpc⁻³.

It is more difficult to estimate precisely the low-redshift volume which has been included to define the low redshift surface brightness, but that volume can be bracketed reasonably well. The most distant galaxy used to define the maximum local starburst surface brightness is NGC 3690, early identified as the most dramatic example of an extended starburst in the Markarian sample of galaxies (Gehrz *et al.* 1983). Taking the Markarian survey as covering 0.25 of the sky and taking the distance of NGC 3690 as 42 Mpc, the volume of the universe examined to find NGC 3690 is 7.5×10^4 Mpc³. The next

closest object in Table 1 is NGC 1068, at 15 Mpc distance. The entire universe has been examined for bright galaxies within that distance, so $1.4 \times 10^4 \text{ Mpc}^3$ has been searched. It is reasonable to conclude that these limits ($1.4 \times 10^4 \text{ Mpc}^3$ to $7.5 \times 10^4 \text{ Mpc}^3$) bracket the local volumes searched to define the maximum surface brightness of nearby extended starburst regions as summarized in Table 1. Based on the 18 sources found in the HDF, we would then expect 7_{-6}^{+12} sources of comparable surface brightness as the HDF high redshift starbursts in the surveyed local volume. In other words, local surveys *do* cover sufficient volume to find the types of high surface-brightness starbursts found in the HDF *if* they are at comparable space densities locally. Using only the 7 objects in Table 1 to define the density of locally-brightest starbursts, the local density of these starbursts is between $9 \times 10^{-5} \text{ Mpc}^{-3}$ and $50 \times 10^{-5} \text{ Mpc}^{-3}$. Because this density range is very similar to that of the (much more luminous) high redshift sample, we also can conclude that extended starburst regions of similar co-moving density have much higher surface brightness at high redshift compared to low redshift.

The result that starburst regions are significantly brighter per unit area at high redshift compared to low redshift is empirical and is our primary conclusion. Understanding why this is the case will require knowing more about the spectral characteristics of starburst regions at high redshift, especially including infrared luminosities. There are two possibilities for explaining this result. The first is that starbursts at high redshift are intrinsically more intense per unit area than are nearby starbursts. The second possibility is that high redshift starbursts are less absorbed by dust, so that a higher proportion of the rest frame ultraviolet escapes and the starbursts simply appear brighter when observed in the rest frame ultraviolet.

Meurer *et al.* (1997) and Pettini *et al.* (1998) conclude that high redshift starburst regions are significantly absorbed, although they differ in conclusions regarding the amount of absorption. Neither suggests a systematic difference between low redshift and high redshift objects, which would discount differing obscuration as the explanation for the differential brightening which we measure. Their efforts to understand the dust absorption in high redshift starbursts were motivated by the importance of understanding the overall rate of star formation at high redshift. This rate can be significantly underestimated if the ultraviolet light of young stars is heavily obscured. Both analyses estimate dust obscuration by the reddening imposed on the ultraviolet spectrum. A difficulty in using only ultraviolet spectra to determine dust obscuration is that all stars which contribute to the ultraviolet luminosity must be assumed to be reddened by an amount small enough that they remain visible but large enough that the effects of reddening are noticeable in the spectrum. Stars which are so obscured that negligible ultraviolet luminosity escapes would not be accounted for. Because of this effect, estimates of obscuration derived strictly from ultraviolet spectra

provide only upper limits for the escaping fraction of ultraviolet luminosity. Accounting for completely obscured stars requires observations in the rest-frame infrared, where the radiation emerges as re-radiation from the obscuring dust (see Rowan-Robinson *et al.* 1997 and Smith *et al.* 1998). Such observations are not available for high redshift starbursts.

The results from Meurer *et al.* yield a distribution of dust obscuration in high redshift starburst regions (their Figure 8), a distribution that can be expressed in terms of the fraction of intrinsic ultraviolet luminosity which escapes. For the present analysis, we wish to know only if this distribution is systematically different compared to low redshift starburst regions. For the low redshift starbursts, we can examine the quantitative obscuration by comparing ultraviolet and infrared luminosities, which together should account for all of the starburst, regardless of the degree of obscuration. This analysis is similar to that in Weedman (1991) but with much improved data. If an IMF is assumed for a starburst and used with stellar atmospheric models describing the ultraviolet luminosity and bolometric luminosity of stars of various masses, the ratio of intrinsic ultraviolet to bolometric luminosity is known for the starburst. For the present analysis, we use the model described in Meurer *et al.* (1997), which normalizes such that $f_{\lambda 2200} = 1.5 \times 10^{-4} f_{\text{bol}}$.

Because of the availability of far-infrared fluxes from IRAS and ultraviolet fluxes from IUE, a substantial number of starburst galaxies have measured bolometric fluxes (Schmitt *et al.* 1997). As these authors comment, there are uncertainties in comparing f_{uv} and f_{bol} because of differing aperture sizes in the observations, but the IUE aperture is large enough that it generally includes all of the relevant starburst, and the IRAS fluxes, though having poorer spatial resolution, are generally dominated by the same starburst regions (Calzetti *et al.* 1995). In Table 3 are given all of the starburst galaxies in Schmitt *et al.* (1997), including those which they classify as both low reddening and high reddening, listing the f_{bol} as read from their plots. Also given are the $f_{\lambda 2200}$ fluxes as deduced from the summary of IUE observations in Kinney *et al.* (1993). (The $f_{\lambda 2200}$ are deduced by interpolating between the entries with central wavelengths of 1913 Å and 2373 Å.) The intrinsic $f_{\lambda 2200}$ deduced from f_{bol} using the Meurer result that $f_{\lambda 2200} = 1.5 \times 10^{-4} f_{\text{bol}}$ is also listed in Table 3. Comparing observed and intrinsic $f_{\lambda 2200}$ yields the fraction of ultraviolet luminosity which escapes, given in the Table.

In Figure 3, the cumulative distributions of escaping fraction for the ultraviolet luminosity are shown. For the median in the distribution of low redshift starbursts from Table 3, only 10% of the intrinsic 2200 Å luminosity escapes. This is similar to the results deduced by Meurer *et al.* (1997) using only the shape of the ultraviolet continuum as an indicator of dust absorption. For their high redshift sample of galaxies, the cumulative distribution is also shown in Figure 3. Comparison of the distributions gives no indication

that a systematically larger fraction of ultraviolet luminosity emerges unobscured from the high redshift starburst regions.

Recall that the obscuration deduced for the high redshift sample is based only on the ultraviolet spectra and could not account for completely obscured stars. The distribution for high redshift, therefore, actually shows upper limits for the escaping fraction of ultraviolet luminosity; the real fraction could be smaller if there are undetected stars because of obscuration. Even so, these upper limits are comparable to the values for the low redshift sample, which *do* account for completely obscured stars. Any systematic difference between the samples arising from the different methods used to estimate obscuration would have underestimated obscuration for the high redshift starburst regions. This is counter to the possible explanation being considered, which requires that high redshift starburst regions have less, not more, obscuration compared to low redshift regions.

The conclusions above indicate that differing dust obscuration does not account for the systematically different surface brightnesses between low redshift and high redshift starburst regions. This is not, however, fully consistent with results reported by Pettini *et al.* (1998). Although they do not present an analysis of individual spectra, Pettini *et al.* conclude that a higher fraction of ultraviolet luminosity escapes in the high redshift galaxies than was concluded by Meurer *et al.* (1997). They report a median dust correction to the ultraviolet luminosity of a factor of 3, although they state it could range from 2 to 6. This dust correction is substantially less than the factor of approximately 10 shown by the distributions in Figure 3. If it is correct that as much as one-third of intrinsic ultraviolet luminosity characteristically escapes from high redshift starburst regions, this would enhance their surface brightness almost enough to account for our observed difference between surface brightnesses of low redshift and high redshift regions (factor of 4 in the median). We note, however, that the Pettini *et al.* results also can only describe an upper limit for escaping ultraviolet luminosity (equivalent to a lower limit to the obscuration factor) because of the absence of any information on bolometric luminosities.

4. Summary

By examining available ultraviolet observations of low redshift starburst regions, we define an upper limit to the surface brightness of such starburst regions as observed on scales of several hundred pc. This limit is 6×10^{-16} ergs cm⁻² s⁻¹ Å⁻¹ arcsec⁻² for rest frame wavelength of 1830 Å. Ultraviolet surface brightnesses at comparable scales for high redshift starburst regions ($z > 2.2$) are measured from galaxies in the Hubble Deep Field. After correcting for cosmological effects, we find that high redshift starbursts have

intrinsic ultraviolet surface brightness that is typically four times brighter than low redshift starbursts.

Because of differing conclusions about the amount of obscuration in high redshift starburst regions, we are left with an ambiguous interpretation as to whether the unexpectedly high surface brightness of starburst regions at high redshift is caused by diminished dust obscuration. If not, some effect is required to make high redshift star formation intrinsically more intense per unit area than star formation in the nearby universe. Either way, our results indicate that something was different on a local scale within starburst regions at redshifts above two compared with those in nearby galaxies, making star formation appear brighter per unit area of a starburst region.

This increased surface brightness may be a significant factor in explaining the increasing luminosity density with redshift observed for ultraviolet-bright galaxies. The distribution with redshift of star-forming galaxies observed in ground-based surveys and in the HDF indicates that the star formation rate per co-moving volume peaks at redshift about unity and remains 5 to 10 times greater than in the nearby universe for $z > 2$ (Madau *et al.* 1996, Lilly *et al.* 1996, Connolly *et al.* 1997). If there is no change in the size or co-moving density of starburst regions, but the star formation intensity per region increases a factor of four, this would be a major factor in explaining the observed differences between the nearby universe and the high redshift universe. In this scenario, the early universe did not require significantly more starburst regions than are observed in the nearby universe, but each region had much more intense (or much less obscured) star formation. Our result is not adequate to prove such a scenario, because this would require that the surface brightness enhancement apply to all starburst regions, whereas our result is able to show this enhancement for only the brightest regions in both nearby and high redshift samples.

DPS acknowledges support from NSF grant AST-9509919. MAB acknowledges support from NASA grant NAG5-6032.

REFERENCES

- Calzetti, D., Bohlin, R.C., Kinney, A.L., Storchi-Bergmann, T., and Heckman, T.M. 1995, ApJ, 443, 136
- Cohen, J. G., Cowie, L.L., Hogg, D.W., Songaila, A., Blandford, R., Hu, E.M., and Shopbell, P. 1996, ApJ (Letters), 471, L5.
- Connolly, A.J., Szalay, A.S., Dickinson, M., Subbarao, M.U., and Brunner, R.J. 1997, ApJ

- (Letters), 486, L11.
- Gehrz, R.D., Sramek, R.A., and Weedman, D.W. 1983, ApJ, 267, 551.
- Kinney, A.L., Bohlin, R.C., Calzetti, D., Panagia, N., and Wyse, R.F.G. 1993, ApJ (Supplement), 86, 5.
- Lilly, S.J., Le Fevre, O., Hammer, F., and Crampton, D. 1996, ApJ (Letters), 460, L1.
- Lowenthal, J.D., Koo, D.C., Guzman, R., Gallego, J., Phillips, A.C., Faber, S.M., Vogt, N.P., Illingworth, G.D., and Cronwell, C. 1997, ApJ, 481, 673.
- Madau, P., Ferguson, H.C., Dickinson, M.E., Giavalisco, M., Steidel, C.C., and Fruchter, A. 1996, MNRAS, 283, 1388.
- Maoz, D., Filippenko, A.V., Ho, L.C., Macchetto, F.D., Rix, H.-W., and Schneider, D.P. 1996, ApJ. (Supplement), 107, 215
- Meurer, G.R., Heckman, T.M., Leitherer, C., Kinney, A., Robert, C., and Garnett, D.R. 1995, AJ, 110, 2665.
- Neff, S.G., Fanelli, M.N., Roberts, L.J., O’Connell, R.W., Bohlin, R., Roberts, M.S., Smith, A.M., Stecher, T.P. 1994, ApJ, 430, 545.
- Rowan-Robinson, M., Mann, R.G., Oliver, S.J., Efstathiou, A., Eaton, N., Goldschmidt, P., Mobasher, B., Serjeant, S.B.G., Sumner, T.J., Danese, L., Elbaz, D., Franceschini, A., Egami, E., Kontizas, M., Lawrence, A., McMahon, R., Norgaard-Nielsen, H.U., Perez-Fournon, I., and Gonzalez-Serrano, J.I. 1997, MNRAS, 289, 490.
- Schmitt, H.R., Kinney, A.L., Calzetti, D., Storchi-Bergmann, T. 1997, AJ, 114, 592
- Smith, D.A., Herter, T., and Haynes, M.P. 1998, ApJ, 494, 150
- Steidel, C.C., Giavalisco, M., Dickinson, M., and Adelberger, K.L. 1996, AJ, 112, 352
- Weedman, D.W. 1991, in Massive Stars in Starbursts, eds: C. Leitherer, N.R. Walborn, T.M. Heckman, C.A. Norman (Cambridge: Cambridge University Press), p. 317
- Williams, R.E., Blacker, B., Dickinson, M., Dixon, W.V., Ferguson, H.C., Fruchter, A.S., Giavalisco, M., Gilliland, R.L., Heyer, I., Katsanis, R., Levay, Z., Lucas, R.A., McElroy, D.B., Petro, L., and Postman, M. 1996, A.J., 112, 1335.
- Zepf, S.E., Moustakas, L.A., and Davis, M. 1997, ApJ (Letters), 474, L1.

TABLE 1
SURFACE BRIGHTNESSES OF BRIGHTEST LOW REDSHIFT EXTENDED STARBURST
REGIONS

Object	Wavelength (Å)	Surface Brightness ^a		Size (pc)	Reference
NGC 1705	1900	4.2	(4.4)	770	b
NGC 3310	1900	3.8	(3.9)	1270	b
NGC 4449	1900	3.6	(3.7)	270	b
NGC 5236	1900	8.6	(8.9)	670	b
NGC 5253	1900	5.3	(5.5)	520	b
NGC 3690-BC	2200	5.0	(6.0)	1300	c
NGC 1068-J	1500	7.0	(5.7)	350	d

^aUnits of 10^{-16} ergs cm^{-2} sec^{-1} Å^{-1} arcsecond^{-2} at the wavelength of the observations; values in parenthesis give surface brightness at the normalized wavelength of 1830 Å, assuming that all objects have ultraviolet spectra of shape $f_\lambda \propto \lambda^{-1}$ (Kinney *et al.*1993).

^bIUE (Kinney *et al.*, 1993)

^cHST FOC (Meurer *et al.*, 1995)

^dUIT (Neff *et al.*, 1994)

TABLE 2
HUBBLE DEEP FIELD HIGH REDSHIFT GALAXIES

Number	Chip	Brightest Pixel		z	S _λ (1830)	Reference
		x	y			
(1)	(2)	(3)	(4)	(5)	(6)	(7)
1	2	647	1740	2.233	4.1	L
2	2	1952	209	2.267	4.4	L
3	4	742	960	2.268	4.9	C
4	2	546	1610	2.419	1.65	L
5	4	279	1321	2.591	3.8	S
6	3	360	1206	2.775	1.61	S
7	4	1586	1172	2.803	4.2	S
8	2	1805	960	2.845	9.1	S
9	4	289	188	2.931	1.24	L
10	4	1952	773	2.980	1.18	L
11	2	356	1299	2.991	2.24	L
12	2	1332	181	3.160	0.82	L
13	2	1281	1738	3.181	1.94	L
14	4	1070	1762	3.226	4.1	S,Z
15	3	330	606	3.233	2.1	L
16	3	506	1279	3.360	0.4	Z
17	2	627	1288	3.368	2.6	L
18	2	620	1219	3.430	1.12	L

NOTE.— (1) Identifying number in Figure 1; (2) WFPC2 chip; (3) x location on HDF image (version 2) of brightest pixel; (4) y location on HDF image (version 2) of brightest pixel; (5) spectroscopic redshift; (6) surface brightness in brightest pixel for rest-frame wavelength of 1830 Å, in units of 10^{-18} ergs cm⁻² s⁻¹ Å⁻¹ arcsec⁻²; (7) reference for spectroscopic redshifts [Lowenthal *et al.*, 1997 (L); Cohen *et al.*, 1996 (C); Steidel *et al.*, 1996 (S); Zepf *et al.*, 1997 (Z)]

TABLE 3
LOCAL STARBURST GALAXIES

Object ^a	f_{bol} ^b	$f_{\lambda 2200}$		Escape Fraction ^e
		Observed ^c	Intrinsic ^d	
Low Reddening				
NGC 5236	145	16.7	220	0.076
NGC 5253	38.9	9.3	58	0.16
NGC 1140	6.0	2.6	9.0	0.29
NGC 7250	4.5	0.81	6.8	0.12
Mrk 960	2.95	1.16	4.4	0.26
NGC 3049	4.17	0.86	6.3	0.13
Mrk 542	2.09	0.39	3.1	0.12
Mrk 357	1.74	0.89	2.6	0.34
UGC 9560	1.58	1.54	2.4	0.65
NGC 6052	7.94	0.92	11.9	0.076
High Reddening				
NGC 1097	57.5	1.74	86	0.02
NGC 3256	102	1.14	153	0.007
NGC 1672	50.1	2.8	75	0.037
NGC 7552	83.2	1.92	125	0.015
NGC 6217	16.6	1.36	25	0.054
NGC 7714	14.1	2.14	21.1	0.10
NGC 4385	6.76	0.97	10.1	0.095
NGC 6090	8.91	0.77	13.4	0.058
IC 214	7.08	0.39	10.6	0.036
NGC 7673	6.61	1.22	9.9	0.123
NGC 5860	3.24	0.42	4.9	0.085
NGC 5996	0.89	0.96	1.34	0.707
IC 1586	2.34	0.42	3.5	0.117
NGC 7793	12.3	0.70	18.5	0.038

^aFor convenience, objects are grouped according to the starburst categories as in Schmitt *et al.* (1997), which they describe as “low reddening” and “high reddening” based on the shapes of the ultraviolet spectra.

^bUnits of 10^{-14} ergs cm^{-2} s^{-1}

^cUnits of 10^{-14} ergs cm^{-2} s^{-1} \AA^{-1}

^dUnits of 10^{-10} ergs cm^{-2} s^{-1} \AA^{-1} . Intrinsic $f_{\lambda 2200} = 1.5 \times 10^{-4} f_{bol}$, from Meurer *et al.* (1997).

^eEscaping fraction = Observed $f_{\lambda 2200}$ / Intrinsic $f_{\lambda 2200}$

Figure Captions

Fig. 1.— Images of the galaxies in Table 1, from the F814W images of the Hubble Deep Field. Each box is $3.32'' \times 3.32''$; each tick mark corresponds to roughly 900 pc ($H_0 = 75 \text{ km s}^{-1} \text{ Mpc}^{-1}$ and $\Omega_0 = 0.2$).

Fig. 2.— Surface brightness (units of $10^{-18} \text{ ergs cm}^{-2} \text{ s}^{-1} \text{ \AA}^{-1} \text{ arcsec}^{-2}$) at 1830 \AA compared to $(1+z)$. Filled triangles: observed values for galaxies in Table 2. Solid curve: expected values for brightest local starburst regions ($6 \times 10^{-16} \text{ ergs cm}^{-2} \text{ s}^{-1} \text{ \AA}^{-1} \text{ arcsec}^{-2}$, see text), faded by cosmological factor of $(1+z)^{-5}$.

Fig. 3.— Normalized cumulative distribution of ultraviolet luminosity which escapes starburst region without being absorbed by dust. Solid line: low redshift starburst regions from Table 3 (24 objects total). Dashed line: high redshift starburst regions from Meurer *et al.* (1997, 23 objects total).

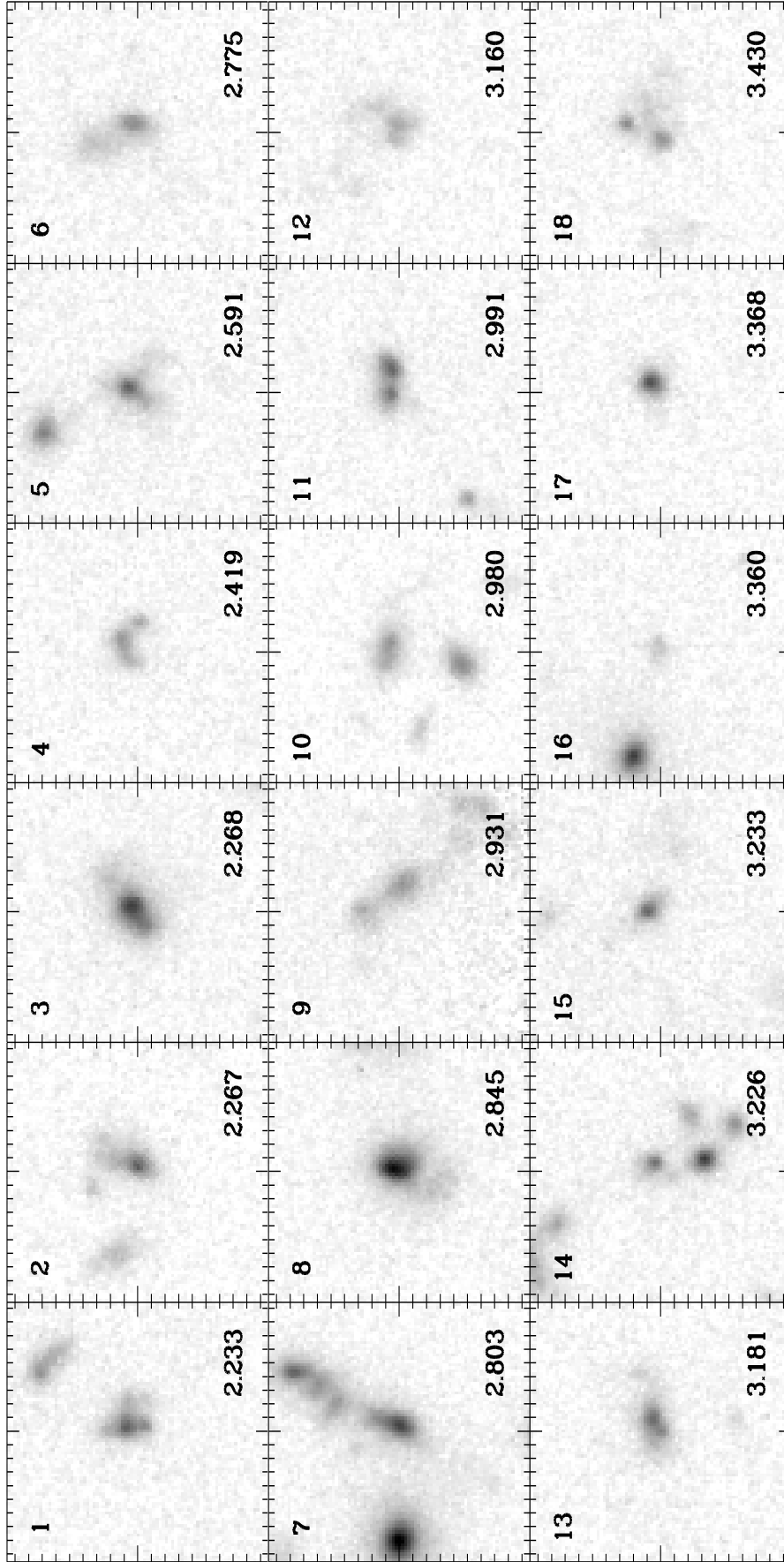


Figure 1 [Weedman et al.]

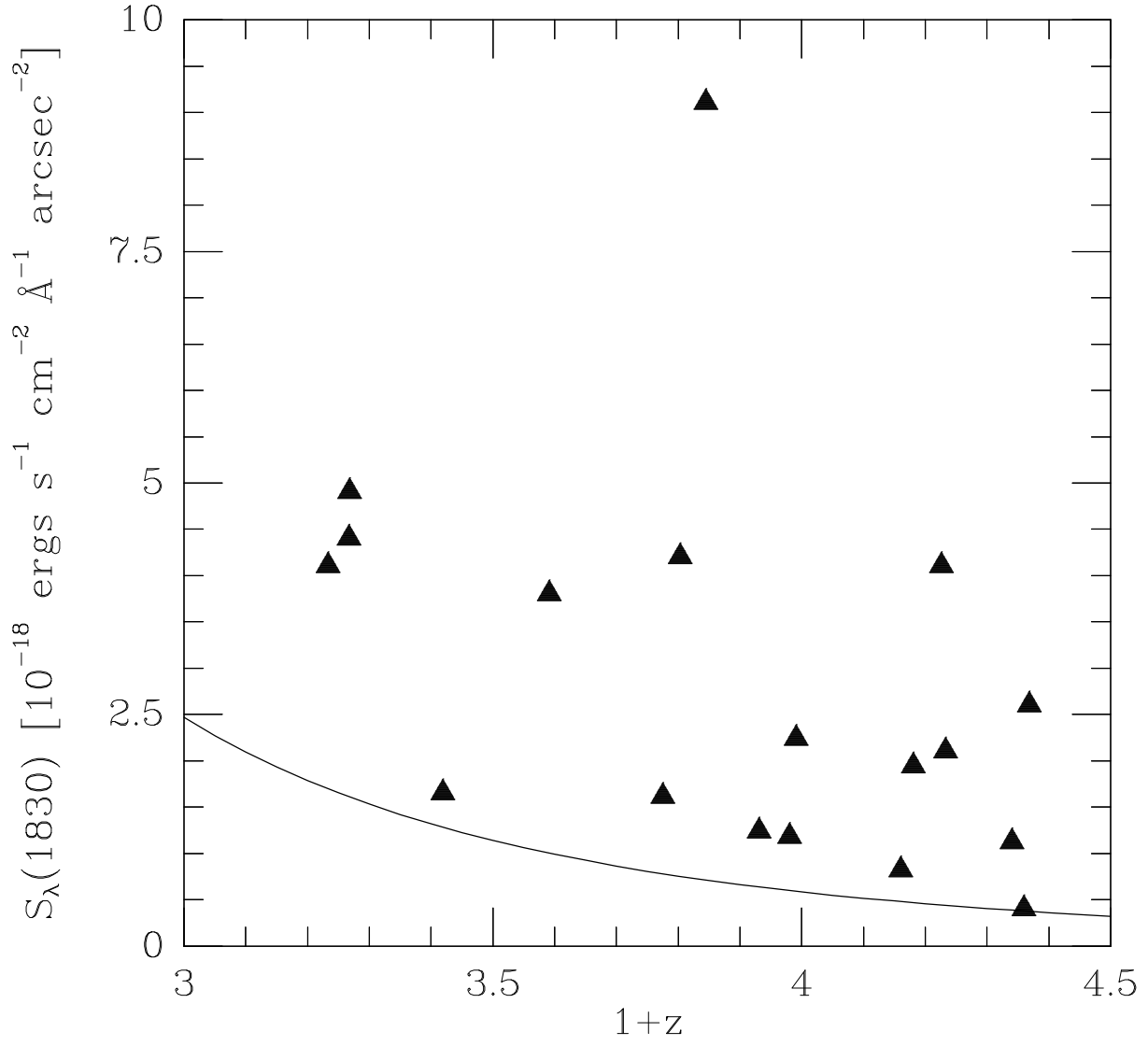


Figure 2

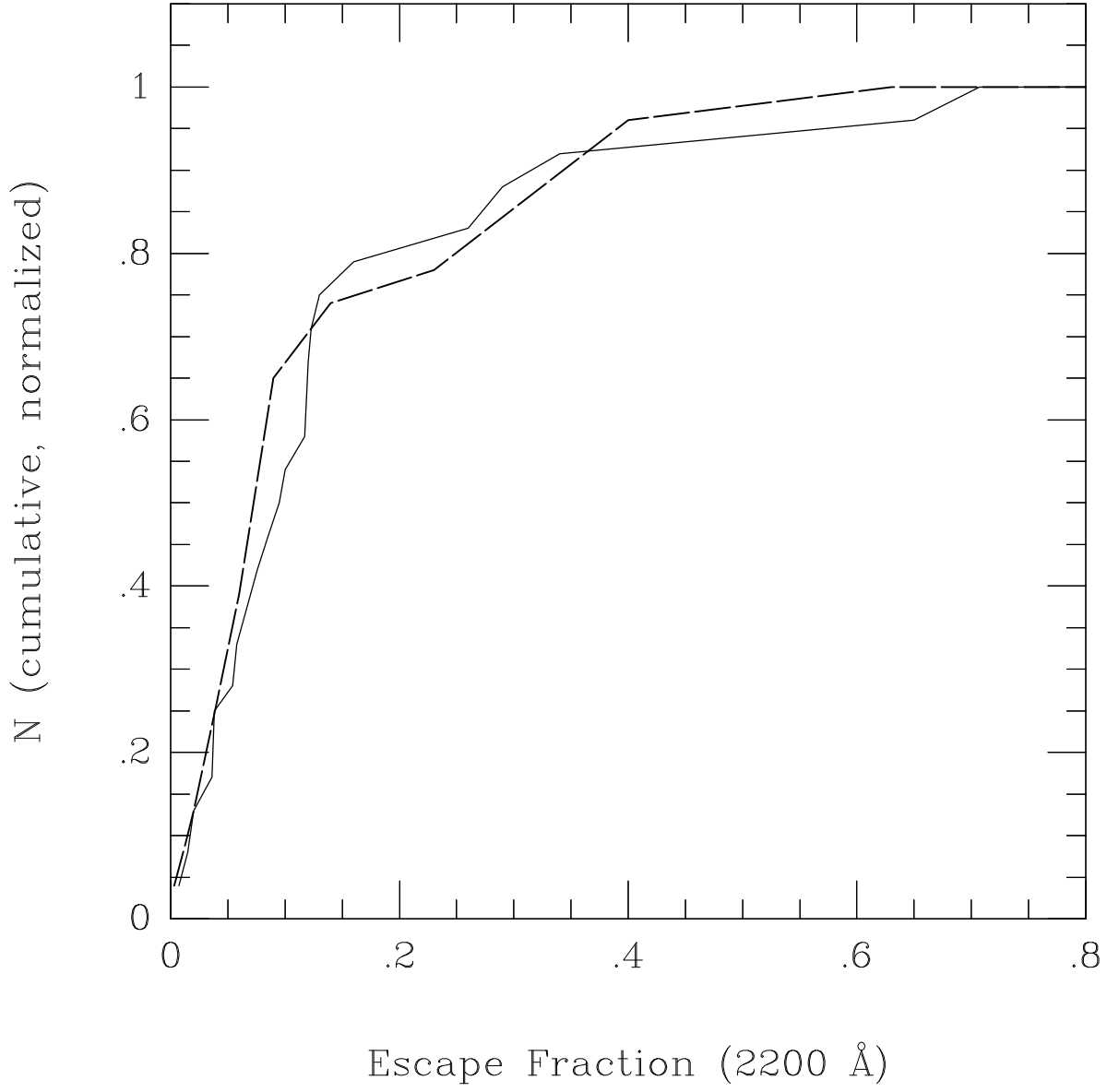


Figure 3